JOURNAL OF MATERIALS SCIENCE 27 (1992) 1772–1780

Microstructure and thermophysical characteristics of $PbTiO_3$-based ceramics

A. AHMAD, S. MIKHAIL, S. CHEHAB, D. OWENS, A. M. TURCOTTE
Ceramic Section, Energy, Mines and Resources, Canada Centre for Mineral and Energy Technology, 555 Booth Street, Ottawa, Canada K1A OG1

Precursor powders of a modified lead titanate-based ceramic material have been synthesized by two different chemical techniques and also by the conventional attrition milling method. The influence of powder processing techniques on the phase development, powder morphology and thermophysical behaviour of the material have been examined. The study shows that the above properties in this material are strongly dependent on the powder synthesis method as well as the thermal treatment of the precursor powders.

1. Introduction

The high-performance characteristics desired in advanced ceramics necessitate the development of new and improved techniques for ceramic powder processing. Conventionally, ceramic bodies are produced by first preparing the precursor powders through mechanical mixing of the chemical ingredients in the form of oxides or carbonates, calcining the powders to decompose the carbonates and to pre-react the material, and finally treating at high temperature to densify and develop mechanical strength through diffusion of the particulates. The major emphasis in conventional processing has been on the physical property control through microstructural development without due attention given to the chemical aspect of the material or processing. This approach causes serious limitations in the control of chemical composition, homogeneity, particle size, shape and other key parameters considered necessary to produce high-performance advanced ceramics, and has contributed to rather limited progress in the field of ceramic science and technology.

It is increasingly being realized that the ceramic powder processing via chemical routes may be the key to produce high-performance advanced ceramics. This is evident from the surge of research activity seen in this area throughout the industrialized world and the tremendous increase in the number of publications that have appeared within the past ten years [1–5]. These studies indicate that the localized variations in the physical chemistry of the surfaces and interfaces within the material can strongly influence the final properties of the ceramic product. Chemical processing can provide manipulation and control of the surfaces and interfaces at the initial stages of the processing at the molecular scale, thus providing more homogeneous materials. It also provides better control over the particle size and shape. The progress in the ceramic powder processing via chemical routes has been very encouraging; a variety of high-performance structural and electromagnetic ceramics with predictable properties, improved reliability and greater resistance to severe environments are being produced using chemically derived ceramic powders [6–9].

Recently, we have been involved in the development of lead titanate-based piezoelectric ceramics via chemical routes [10]. The growing interest in this material is because of its low dielectric constant (~ 200), high Curie temperature ($> 250\,^{\circ}C$), a large difference between the thickness coupling constant, k_t, and planar coupling constant, k_p, and relatively low mechanical quality factor, Q_m., These characteristics make it a promising candidate for high-frequency ultrasonic transducer applications. However, difficulties are encountered in the sintering and subsequent poling of $PbTiO_3$ due to the high anisotropy in its crystal structure (large c/a ratio), which leads to the development of micro- and macrocracks upon sintering and subsequent cooling through the Curie point. Doping with alkali metals, transition metals or rare-earth oxides has been shown to produce crack-free high-density material [11–14]. In an earlier study [10] we reported the synthesis and characterization of calcia-doped lead titanate compositions having a general formula $[Pb_{1-x}Ca_x][(Co, W)_yMn_zTi_{1-2y-z}]O_3$, where $x \leqslant 0.35$, $y \leqslant 0.03$, $z \leqslant 0.01$. Two different chemical routes and also conventional attrition milling methods were used to synthesize the precursor powders. The influence of powder processing methods on the crystal structure, unit cell parameters and the particle size/surface area were discussed. It was observed that gel processing can furnish virtually single-phase $PbTiO_3$ at temperatures above $600\,^{\circ}C$. However powders produced by attrition milling and chemical co-precipitation contained impurity phases even when heat treated to $800\,^{\circ}C$. This study provides data on the microstructural characteristics and thermophysical behaviour of the powders. It also shows how minor

0022–2461

variations in the processing conditions can improve the structural characteristics of the chemically derived powders.

2. Experimental procedure

A schematic diagram showing the powder preparation methods for modified lead titanate composition is given in Fig. 1. For gel-processing, appropriate amounts of $PbCO_3/Pb(CH_3COO)_2 \cdot 3H_2O$, calcium, cobalt and manganese acetates were dissolved in 80% aqueous acetic acid. Titanium-*N*-tetra butoxide (TNBT) also dissolved in 80% aqueous acetic acid, was then added dropwise to the above mixture to give a pink solution. This solution was evaporated in a rotary vacuum flask at $\sim 40\,^{\circ}C$ to form a viscous gel. The gel was subsequently precipitated in isopropanol and splat dried at 125 °C to give bluish grey powders.

For chemical coprecipitation, lead, calcium, cobalt and manganese acetates were dissolved in a minimal amount of water at $\sim 60\,^{\circ}C$. TNBT was dissolved in excess oxalic acid forming a yellow solution and this solution was then added dropwise to the acetates to form pinkish precipitates. The precipitation was completed by adding concentrated ammonium hydroxide to a pH of 8.5. The mixture was evaporated in a rotary vacuum flask and oven dried at 125 °C.

The conventional approach involved wet attrition milling the raw materials in the form of oxides or carbonates for 4 h followed by vacuum filtration of the slurry and subsequent oven drying at 125 °C. Details of the powder synthesis are given elsewhere [10].

Powders were calcined in small batches (< 10 g) in alumina crucibles loosely covered with platinum foil at temperatures ranging from 150–800 °C. The samples were kept at the desired temperature for a period of 2 h and allowed to cool to room temperature by turning off the furnace. X-ray diffraction patterns for these powders were obtained using a Rigaku automated powder diffractometer with CuK_α radiation and a graphite monochromator.

For the study of the thermal behaviour of the precursor powders, a DuPont 9900TA thermal analysis system with 951 TGA and high-temperature DTA module was used. All the samples were examined in both air and nitrogen atmosphere using a heating rate of $10\,^{\circ}C\,min^{-1}$. In some experiments, concurrent TG/DTA technique was used. This technique was explained in detail earlier [15].

3. Results and discussion

3.1. X-ray diffraction studies

The XRD data in our earlier work [10] indicated that the development of phases in all three powders is strongly influenced by both the powder preparation methods and the calcination temperatures. The gel-derived material produced virtually single phase $PbTiO_3$ (with only trace amounts of PbO) at 500 °C. However, both coprecipitated and attrition-milled powders displayed the presence of substantial amounts of impurity phases, i.e. PbO, TiO_2 and $CaCO_3$ along with $PbTiO_3$ even after heat treating to 800 °C. The presence of unwanted impurity phases was rather intriguing, especially for powders produced via the chemical coprecipitation method. It was therefore decided to analyse the mother liquor (obtained after vacuum filtration) of the coprecipitated mixture via inductively coupled plasma spectroscopy (ICPS). The ICPS data indicated the presence of metallic

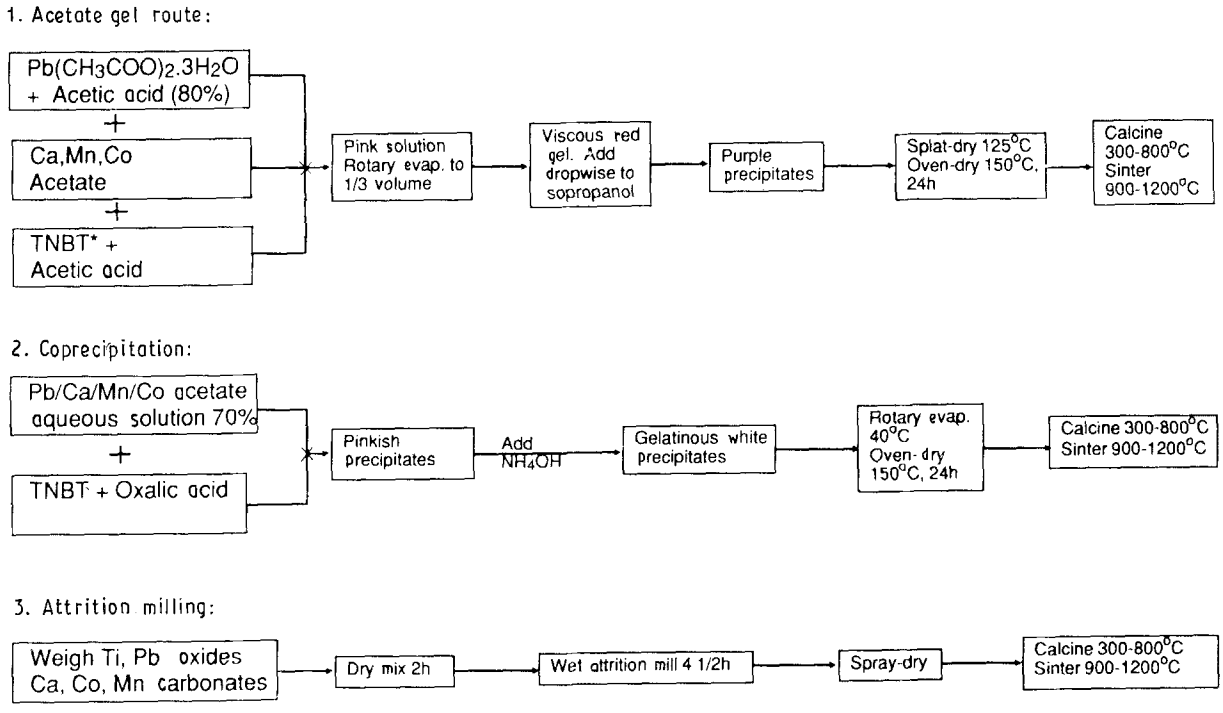

Figure 1 A schematic diagram for powders prepared by (1) gel-processing, (2) chemical coprecipitation, and (3) attrition milling.

cations in the mother liquor after the precipitation. The quantities present correspond to losses of 0.1% Ca, 31.7% Co, 72.7% Mn, 0.4% Pb and 1.7% Ti, and are sufficient to warrant concerns about changes in the elemental composition of the precipitate. Large losses seem to be confined to the transition metals, which may be due partly to their small concentrations and partly to amino-cation complexation, which tends to result in soluble cation complexes. A new batch of the coprecipitated material was therefore prepared by evaporation of the coprecipitated mixture in a rotary flask under vacuum at ~ 40 °C so that losses during filtration process could be avoided. The new material when heat treated to 600 °C showed remarkable improvement over the previous batch (Fig. 2). Virtually single-phase lead titanate was produced after heat treatment of the rotary-evaporated powder, whereas vacuum-filtered material displayed considerable amounts of undesirable phases.

In our earlier work, we also reported that gel-derived material clearly showed $PbTiO_3$ formation at 500 °C. However, this material continued to show trace amounts of PbO even upon heat treating the material at 700 °C. This process was therefore slightly modified by using lead acetate trihydrate as one of the raw materials as opposed to lead carbonate used in our earlier work. This modification provided improved precursor raw material, as heat treatment of these powders to 500 °C produced single-phase $PbTiO_3$, Fig. 3a, b. Unlike the previous batch (Fig. 3a) the XRD patterns of the new material did not display any undesirable PbO phases (Fig. 3b).

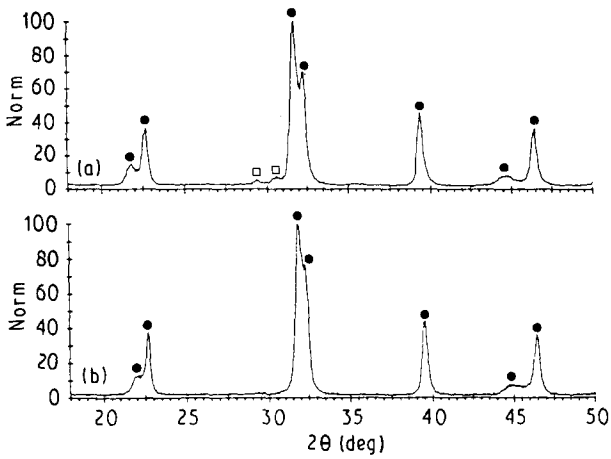

Figure 3 XRD patterns of the precursor powders produced by the gel-processing method and heat-treated to 500 °C using (a) $PbCO_3$, (b) $Pb(CH_3COO)_2 \cdot 3H_2O$ as raw materials. (●) $PbTiO_3$, (□) PbO(O).

3.2. Microstructure

The scanning electron micrographs of the gel-derived, coprecipitated and attrition-milled powders heat treated at temperatures of 100, 500 and 750 °C are shown in Figs 4–6.

At 100 °C, gel-derived powders contained broken pieces of dried gel (Fig. 4) ranging in sizes from 1–150 μm. The particles are irregular in shape and have smooth surfaces. Some of the larger particles exhibit distinct conchoidal fractures. At 500 °C the particles appeared glazed. The particle size ranged from 1–100 μm; the interior surfaces of many of the larger particles exhibited microcracks and microporosity which could explain the observed high surface area in these powders [10]. These particles also showed numerous inclusions of what may be a glass phase. These powders could be easily hand crushed to particles of less than 5 μm size. At 750 °C, the agglomerates were sintered into harder pieces. The general appearance of the particles is similar to those calcined at 500 °C. Most grains have a smooth glass-like surface and exhibit microporosity and microcracking. A closer examination of the material reveals the formation of $PbTiO_3$ crystals in a glassy-type matrix.

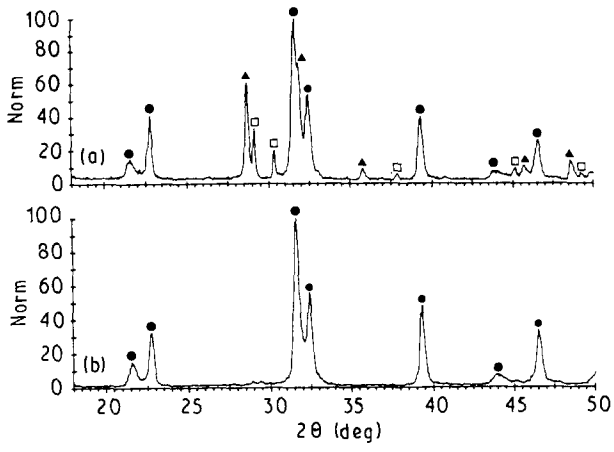

Figure 2 XRD patterns of the precursor powders produced by chemical coprecipitation and heat-treated to 600 °C, with solvent removed by (a) vacuum filtration, (b) by rotary evaporation. (●) $PbTiO_3$, (▲) PbO(T), (□) PbO(O).

Green discs made from the powders (calcined at 750 °C) could not be sintered to > 90% theoretical density. However, after attrition milling this material for 30–45 min the sintered densities of the pellets improved significantly (> 97%). This is due to the removal of internal micro-porosity in the particles attained via attrition milling.

The powders produced by chemical coprecipitation and dried at 100 °C consist of minute particles, small aggregates and larger fused lumps with maximum size of 0.5 mm (Fig. 5). There is no crystal form evident and, as opposed to the gel-derived powders, the surfaces of particles are not smooth. At 500 °C, irregularly shaped particles and small lumps ranging between 5 μm and 0.7 mm in size are observed. Those in excess of 10 μm are usually multiphase. They often consist of severely cracked matrix containing numerous inclusions of PbO and an apparent glass phase. The principal element in the glass phase is titanium; however, the glass contains more lead and much more calcium than does the matrix. Several agglomerates are found to contain PbO inclusions in a titanium-rich lead oxide matrix. The powders calcined at 750 °C consist of particles of lead titanate ranging from 1–100 μm in size. Some of the agglomerates have an almost granular appearance and a few of the smaller agglomerates

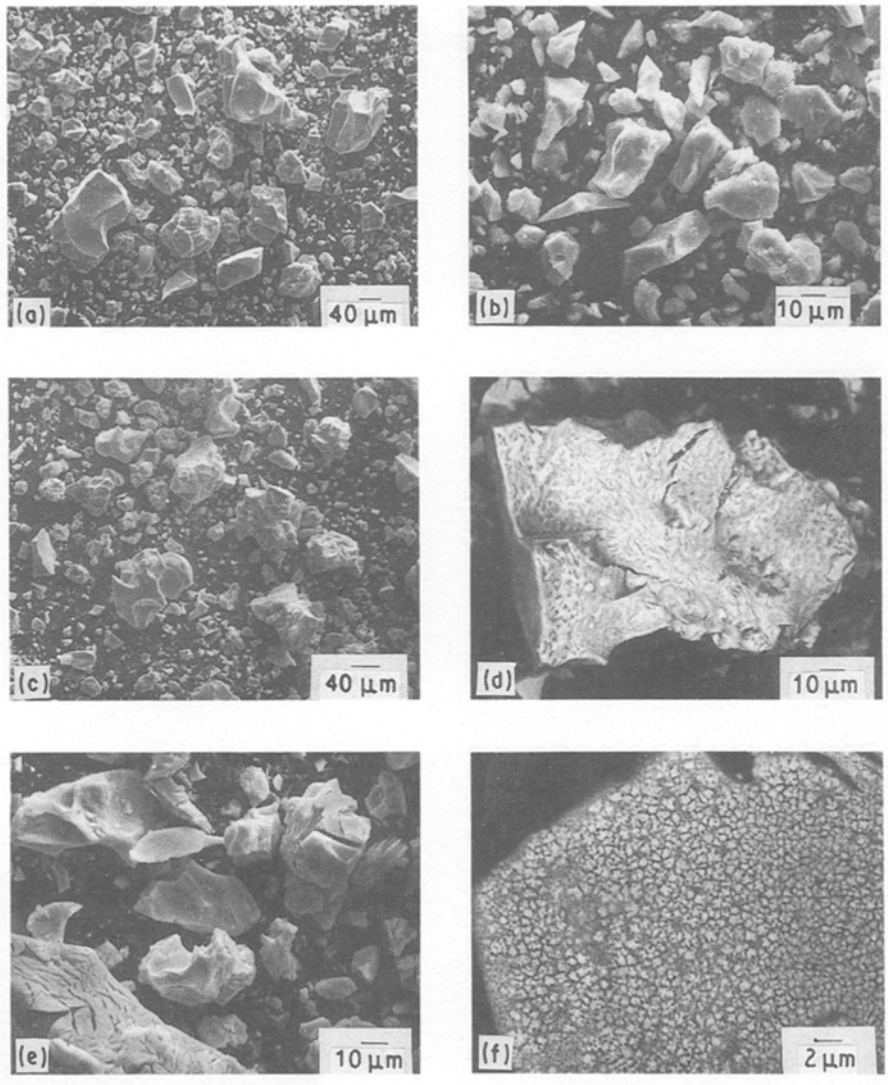

Figure 4 Scanning electron micrographs of gel-derived precursor powders heat treated to (a, b) 100 °C, (c, d) 500 °C and (e, f) 750 °C.

have elongated platelets of PbO indicating compositional inhomogeneity. Like gel-processed materials these powders also require attrition milling for 30–45 min to produce pellets having densities in excess of 97% theoretical.

The powders produced via attrition milling and dried at 100 °C consist of irregularly shaped particles of < 6 μm size. There is considerable phase inhomogeneity as evinced from the SEM (Fig. 6). At 500 °C, most of the particles are discrete, although some agglomerates are visible. Many of the particles are smaller than 1 μm and a few are larger than 5 μm. Most of the larger particles are platy PbO. The smaller grains are generally lead titanium oxide containing small amounts of calcium. At 750 °C, the powders mainly consist of $PbTiO_3$ crystals bound together. The individual grains are from 0.5–4 μm. Only trace amounts of PbO are detected. It was impossible to produce sintered discs of $> 95\%$, even after re-attrition milling for 1 h using these powders.

3.3. DTA/TGA studies

In the preliminary work, individual starting materials used in the preparation of the precursor powders were first examined by thermal analysis. Fig. 7 shows the TG/DTA diagrams for lead acetate in air. A small weight loss on the TG diagram and an endothermic peak on the DTA diagram appeared at low temperature, signifying the evolution of absorbed H_2O. The melting of anhydrous lead acetate appeared as an endothermic peak around 200 °C with no corresponding change in weight [16]. Above 230 °C, at least three stages of weight loss, accompanied by overlapping exothermic and endothermic peaks, appeared on the diagrams. The first stage of weight loss is due to the decomposition of lead acetate which may take place according to the following scheme:

$$Pb(CH_3COO)_2 = PbCO_3 + (CH_3)_2CO \quad (1)$$

The appearance of an exothermic peak during this reaction is probably due to the oxidation of the evolved acetone in the gas phase. The succeeding stages of weight loss in the temperature range 280–380 °C correspond to the decomposition of the carbonate as follows [17]:

$$2PbCO_3 = PbO \cdot PbCO_3 + CO_2 \quad (2)$$

$$3(PbO \cdot PbCO_3) = 2(2PbO \cdot PbCO_3) + CO_2 \quad (3)$$

$$2PbO \cdot PbCO_3 = 3PbO + CO_2 \quad (4)$$

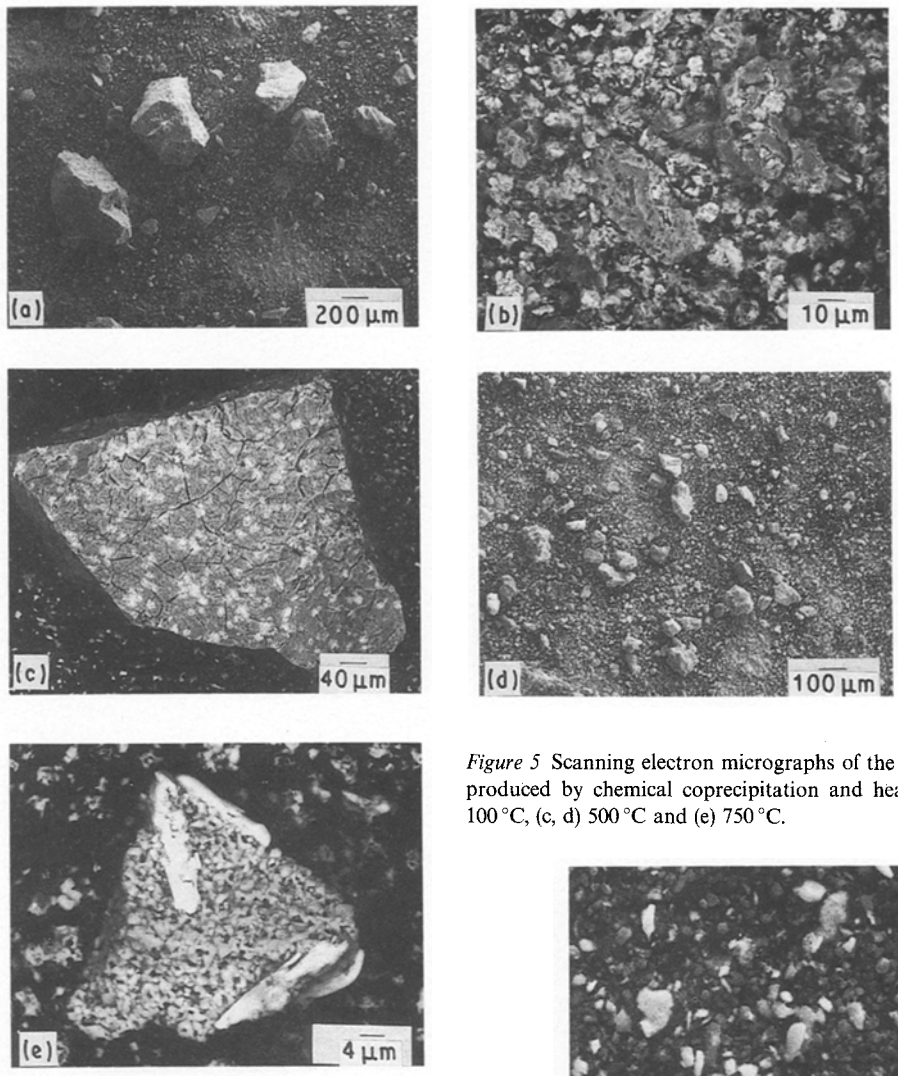

Figure 5 Scanning electron micrographs of the precursor powders produced by chemical coprecipitation and heat treated to (a, b) 100 °C, (c, d) 500 °C and (e) 750 °C.

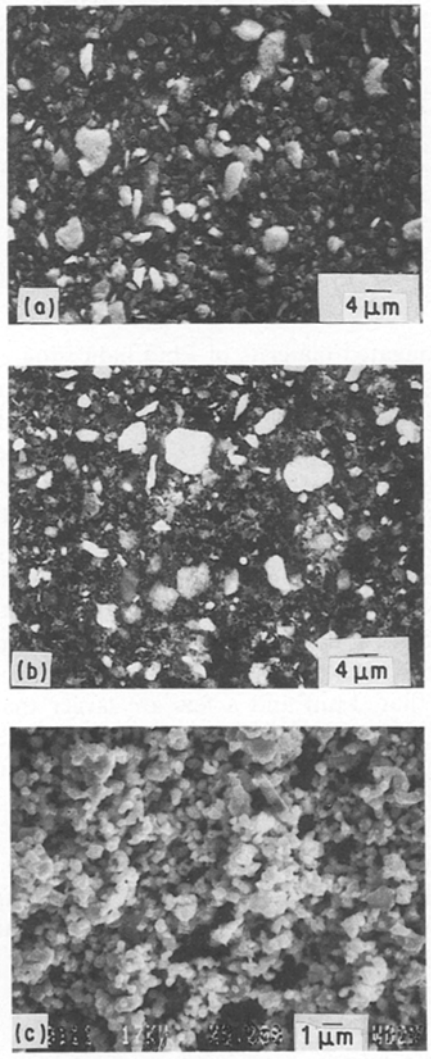

Figure 6 Scanning electron micrographs of the precursor powders produced by attrition milling and heat treated to (a) 100 °C, (b) 500 °C and (c) 750 °C.

In the presence of oxygen, the PbO produced by Reaction 4 oxidizes almost immediately to Pb_3O_4 which decomposes again to the monoxide at temperatures above 550 °C [17] (not shown on the figures).

Fig. 8 shows TG/DTA diagrams for lead acetate in nitrogen. It is evident that the figures are similar to those in air except for the absence of the exothermic peak related to the oxidation of acetone and hence the appearance of the endothermic peaks of the decompositions. It is also observed that the final weight in nitrogen is slightly less than in air as a result of the formation of PbO rather than Pb_3O_4 as a final product. The decomposition of lead carbonate in air and in nitrogen was verified quantitatively in separate experiments.

TG/DTA diagrams for the decomposition of calcium acetate in air are shown in Fig. 9. A two-step weight loss and corresponding endothermic peaks in the temperature range 150–220 °C indicated the release of water of crystallization. A small endothermic peak which appeared at 270 °C, with no corresponding change in weight, is due to a solid state transformation in the anhydrous acetate [18]. A major weight loss due to the decomposition of the acetate commenced at 420 °C. A change in the rate of weight loss, observed during the decomposition process, has been related to the melting of the acetate [19]. In the

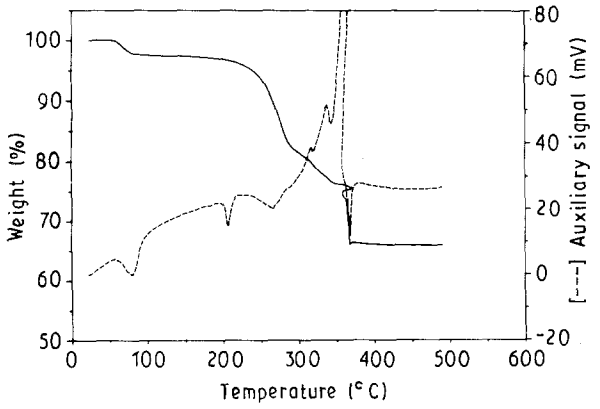

Figure 7 Concurrent TG/DTA diagrams for lead acetate in air.

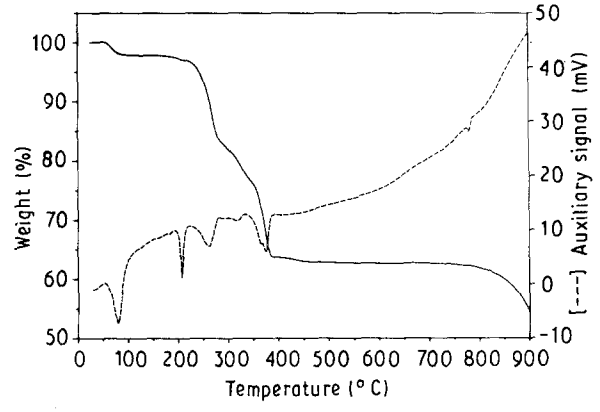

Figure 8 Concurrent TG/DTA diagrams for lead acetate in nitrogen.

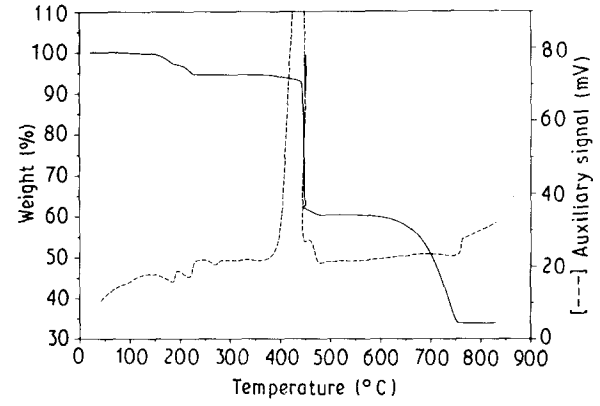

Figure 9 Concurrent TG/DTA diagrams for calcium acetate in air.

DTA figure, endothermic peaks due to the decomposition and melting overlapped with exothermic peaks generated by the oxidation of acetone. The latter was generated during the decomposition reaction

$$Ca(CH_3COO)_2 = CaCO_3 + (CH_3)_2CO \quad (5)$$

At higher temperatures (> 600 °C), the carbonate decomposes to the oxide as shown by the weight loss and accompanying endothermic peak

$$CaCO_3 = CaO + CO_2 \quad (6)$$

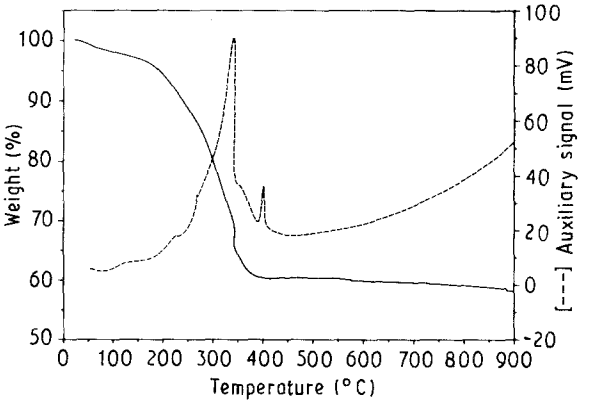

Figure 10 Concurrent TG/DTA diagrams for TNBT (acetate) in air.

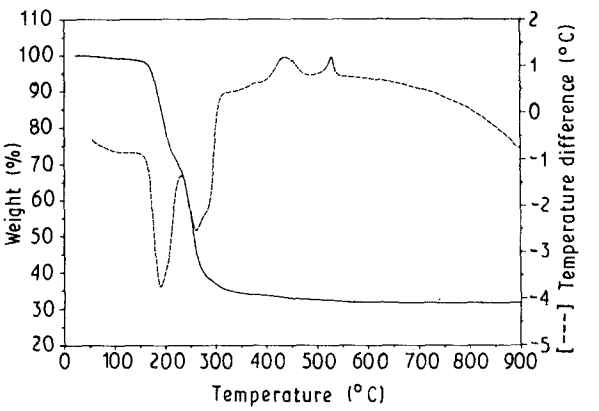

Figure 11 TG/DTA diagrams for TNBT (oxlate) in air.

The decomposition of calcium acetate in nitrogen was also examined and, as in the case of lead acetate, the only significant difference was the absence of the exothermic peak related to the oxidation of acetone in the gas phase.

Samples from two titanium tetrabutoxide-based compounds were also examined. The first compound was prepared by mixing TNBT with acetic acid and precipitating with isopropanol. TG/DTA diagrams for this sample (in air) are shown in Fig. 10. A major weight loss accompanied by an exothermic peak due to the oxidation of acetone in the gas phase, occurred between 200 and 380 °C. A smaller exothermic peak with no corresponding change in weight, typical for the crystallization of amorphous material, appeared on the diagram at 400 °C. The product was identified by XRD as TiO_2. The compound was also examined in nitrogen and the main differences were the absence of the acetone oxidation peak and the slightly higher temperature of crystallization (430 °C).

The second compound was prepared by mixing TNBT with oxalic acid and precipitating with ammonium hydroxide. In air (Fig. 11), an extensive multistage weight loss accompanied by major endothermic peaks occurred in the temperature range 160–320 °C. This may be due to a dehydration step followed by the decomposition of the oxalate to carbonate and then to the oxide. Two more exothermic peaks, with no accompanying weight loss, appeared on the DTA diagram at 440 and 540 °C. The first may be due to the

recrystallization of the dehydration–decomposition product and the second to the polymorphic transformation of anatase TiO_2 to the high-temperature form, rutile. The final product was identified by XRD as rutile. In nitrogen, the material showed similar thermal behaviour to that in air except for the shifting of the polymorphic transformation peak to a somewhat higher temperature (580 °C). The peak was also smaller than that in air which indicated that only partial transformation may have taken place. An XRD analysis indicated that the product was a mixture of anatase and rutile TiO_2. A study of the anatase/rutile transformation was published earlier by Shannon and Pask [20].

3.4. Acetate-based precursor

The TG/DTA diagrams for the Ti–Pb–Ca acetate-based precursor in air are shown in Fig. 12. A minor weight loss below 100 °C due to loss of moisture and a major weight loss from 220–360 °C due to the decomposition of TNBT and lead carbonate appeared on the TG diagram. Another minor weight loss due to the decomposition of $CaCO_3$ appeared around 650 °C. In the DTA figure, an endothermic peak followed by a major exothermic one in the temperature range 220–360 °C verified the decomposition reactions as well as the oxidation of one of the main products, acetone, in the gas phase. Two smaller exotherms at 450 and 530 °C may be due to the oxidation of acetone produced by the decomposition of calcium acetate and the oxidation of PbO (the product of the decomposition of $PbCO_3$) to Pb_3O_4. The latter decomposes again to PbO around 550 °C. A minor endothermic peak due to the decomposition of $CaCO_3$ appeared around 680 °C. Despite the absence of other significant thermal effects, the formation of $PbTiO_3$ from PbO and TiO_2 [21] and the crystallization of amorphous $PbTiO_3$ [22, 23] are known to occur at 500–650 and 450–600 °C, respectively.

The acetate-based precursor was also examined in a nitrogen atmosphere and the resulting TG/DTA figures are shown in Fig. 13. The weight loss trend is essentially the same as that in air. The DTA diagram, however, is characterized by the absence of the major oxidation peak around 300 °C as well as the minor

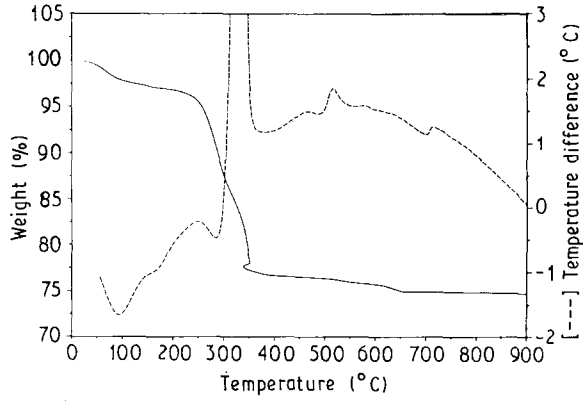

Figure 12 TG/DTA diagrams for the acetate-based precursor in air.

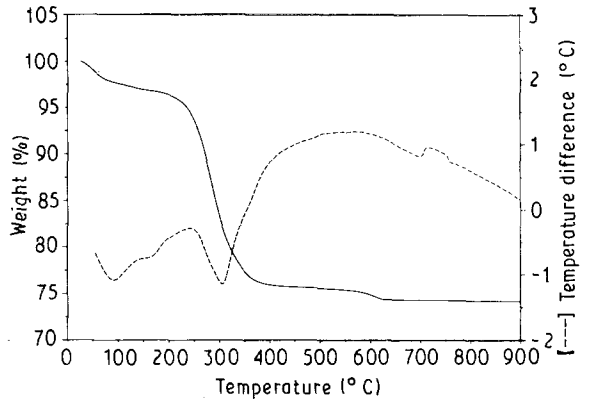

Figure 13 TG/DTA diagrams for the acetate-based precursor in nitrogen.

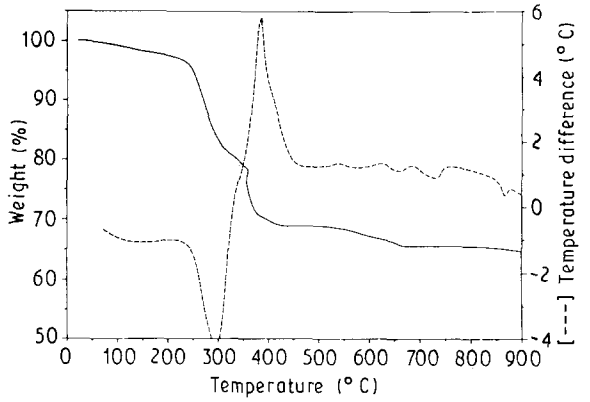

Figure 14 TG/DTA diagrams for the oxolate-based precursor in air.

ones at 450 and 530 °C. The final product of the experiments in air and in nitrogen atmospheres was identified by XRD as $PbTiO_3$.

3.5. Oxalate-based precursor

Fig. 14 shows TG/DTA curves for the Ti–Pb–Ca oxalate-based precursor in air. This material was precipitated using ammonium hydroxide. A multi-stage weight loss accompanied by a major endothermic and a major exothermic peak appeared on the TG and DTA diagrams in the temperature range 230–430 °C. These activities correspond to the dehydration of titanium oxysalts (probably oxalates) and the decomposition of the anhydrous product to the carbonate and further to the oxide. The complex exothermic peak at 350–450 °C may be mainly due to the oxidation of evolved acetone, produced during the decomposition of lead and calcium acetates, in the gas phase. Although the starting material is crystalline in nature, the dehydration/decomposition process may produce an amorphous product that recrystallizes at a higher temperature. This may also account partially for the observed exothermic activities on the DTA diagram. Between 500 and 750 °C, minor weight loss accompanied by thermal activities on the diagrams may relate to an oxidation/decomposition of PbO, the formation of $PbTiO_3$ (no change in weight), and the decomposition of $CaCO_3$. A minor endothermic

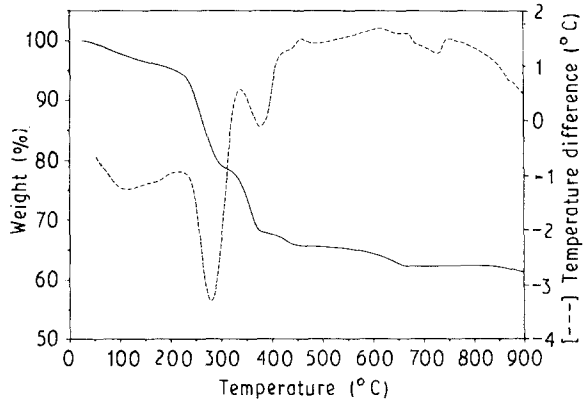

Figure 15 TG/DTA diagrams for the oxolate-based precursor in nitrogen.

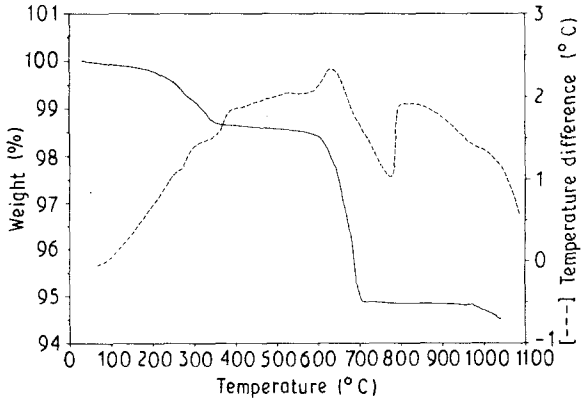

Figure 17 TG/DTA diagrams for the attrition-milled precursor in nitrogen.

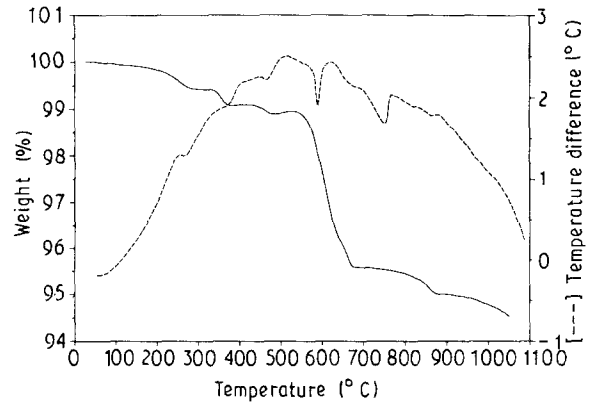

Figure 16 TG/DTA diagrams for the attrition-milled precursor in air.

peak at 870 °C on the DTA diagram indicated the presence of excess PbO (m.p. 886 °C).

The same material was examined in a nitrogen atmosphere, Fig. 15. The TG figure was similar in form to that obtained in air. The DTA diagram, however, was somewhat different. An endothermic peak due to the decomposition of the contained lead and calcium acetates appeared in place of the exothermic peak (in air) of the oxidation of gaseous acetone; a small exothermic peak which may be due to the crystallization of the amorphous material following the dehydration/decomposition reactions appeared in the figure at 430 °C; the minor exothermic peak due to the oxidation of PbO (at 530 °C in air) did not appear.

3.6. Attrition-milled material

This material was mainly composed of lead oxide, titanium oxide and calcium carbonate. The compounds were mechanically mixed in distilled H_2O and attrition milled. Fig. 16 shows the TG/DTA diagrams of the material in air. An initial weight loss of about 1.0% in the temperature range 200–380 °C appeared on the TG diagram accompanied by an endothermic peak on the DTA figure indicating the removal of the water of hydration from the constituent compounds and possibly the decomposition of minor amounts of basic lead carbonate ($2PbCO_3 \cdot Pb(OH)_2$) formed during the attrition-milling process. In air, the latter material is likely to decompose to Pb_3O_4 which, in turn, decomposes to PbO around 580 °C as evinced by the weight loss and the endothermic peak observed at this temperature. Also in the temperature range 550–700 °C, the decomposition of $CaCO_3$ (weight loss and an endothermic peak) and the formation of $PbTiO_3$ (an exothermic peak) seem to have taken place. Above 850 °C the weight loss in the TG figure and the endothermic drift on the DTA diagram can be related to melting and volatilization of excess PbO in the sample.

Fig. 17 shows the TG/DTA diagrams of the same material in nitrogen. An initial weight loss slightly larger than that in air occurred in the same temperature range (200–400 °C). The larger weight loss together with the absence of the endothermic peak (at 580 °C) of the decomposition of Pb_3O_4 implied the formation of PbO rather than Pb_3O_4 as in the case of air. It is also noticeable that the minor exothermic peak related to the formation of $PbTiO_3$ appeared at somewhat lower temperature (630 °C) than that in air (670 °C). At higher temperature, melting and volatilization of excess PbO was evident from the weight loss in the TG figure and endothermic change on the DTA diagram. After the thermal analysis in air and in nitrogen, the samples were found to be sintered, which is expected as a result of the melting of PbO.

The results obtained for the attrition-milled precursor were verified by examining reagent-grade PbO and a mixture of PbO and TiO_2 by thermal analysis in air and in nitrogen.

4. Conclusions

The results from the above studies indicate that the undesirable phases in coprecipitated powders can be avoided using a rotary evaporation technique for solvent removal instead of vacuum filtration. The rotary evaporation technique inhibits the loss of soluble cations in the mother liquor thus maintaining the stoichiometry of the mixture and eliminating the formation of unwanted phases as indicated from the XRD data. Both gel-processed and coprecipitated materials can be heat treated to produce single-phase

lead titanate at temperatures above 500 °C. However, the conventionally attrition-milled powders continued to display trace amounts of PbO at temperatures as high as 800 °C [10]. This suggests that compared to conventional attrition milling, chemical processing can furnish a superior product at relatively lower calcination temperatures.

The SEM studies indicate that, compared with conventional attrition milling, the chemically derived powders contain highly agglomerated large particles (maximum size $\sim$ 500 μm as opposed to 5 μm for attrition-milled material). However, the chemically derived material can easily be crushed to yield submicrometre particle size that can provide high-density sintered discs (> 97% theoretical). When heat-treated, chemically derived powders display microporosity and microcracking presumably due to the decomposition of the organics which may explain the observed high surface area of these powders [10]. The chemically derived powders also exhibit a titania-rich glassy phase that may be responsible for the observed higher sintered densities compared with the attrition-milled material.

The thermophysical behaviour of the ceramic precursor powders appears to depend on the method of synthesis and the prevailing atmosphere. On heating, the acetate-based and oxalate-based starting mixtures decomposed via different routes to form lead titanate. In air, the decomposition was highly exothermic (particularly for the acetate-based precursor) due to the oxidation of volatile decomposition product in the gas phase. The formation of lead titanate was also verified when an attrition-milled precursor powder was heat treated in air or nitrogen. The thermal behaviour of this powder was also slightly different from that in nitrogen due to the formation of Pb_3O_4 and its subsequent decomposition back to PbO below 600 °C.

Acknowledgements

The authors acknowledge the technical assistance of their colleagues in the Mineral Sciences Laboratories, E.M. and R., CANMET, in particular Ms K. Besso and Mr P. Carriere for providing XRD data on the powders, and Mr A. G. McDonald for powder preparations. The authors also thank Dr A. K. Kuriakose and Dr T. A. Wheat, Mineral Sciences Laboratories, for very stimulating and invaluable discussions throughout the course of this work.

References

1. C. J. BRINKER, D. E. CLARK and D. R. ULRICH, in "Better Ceramics Through Chemistry", Material Research Society Symposium Proceedings, Vol. 32 (Material Research Society, 1984).
2. *Idem.*, in "Better Ceramics Through Chemistry II", Material Research Society Symposium Proceedings, Vol. 73 (Material Research Society, 1986).
3. *Idem.*, in "Better Ceramics Through Chemistry III", Material Research Society Symposium Proceedings, Vol. 121 (Material Research Society, 1988).
4. L. L. HENCH and D. R. ULRICH, "Ultrastructure Processing of Ceramics, Glasses and Composites" (Wiley, New York, 1984).
5. J. D. MACKENZIE and D. R. ULRICH, "Ultrastructure Processing of Advanced Ceramics" (Wiley, New York, 1988).
6. S. R. GURKOVICH and J. B. BLUM, *J. Mater. Sci.* **20** (1985) 4479.
7. K. D. BUDD, S. K. DEY and D. A. PAYNE, in "Special Proceedings of British Ceramic Society on Electronic Ceramics" (British Ceramic Society, Stoke-on-Trent, 1984) p. 123.
8. D. W. JOHNSON Jr, *J. Amer. Ceram. Soc. Bull.* **60** (1981) 221.
9. J. H. CHOY, J. S. YOO, S. G. KANG, S. T. HONG and D. G. KIM, *Mater. Res. Bull.* **25** (1990) 283.
10. A. AHMAD, K. BESSO, S. CHEHAB, T. A. WHEAT and D. NAPIER, *J. Mater. Sci.* **25** (1990) 5298.
11. I. UEDA and S. IKEGAMI, *Jpn J. Appl. Phys.* **7** (1968) 236.
12. S. IKEGAMI, I. UEDA and T. NAGATA, *J. Acoust. Soc. Amer.* **50** (Part 1) (1971) 1060.
13. I. UEDA, *Jpn J. Appl. Phys.* **11** (1972) 450.
14. Y. YAMASHITA, K. YOKOYAMA, H. HONDA and T. TAKAHASHI, *ibid.* **20** Supplement 20-4 (1981) 183.
15. S. A. MIKHAIL, *Thermochim. Acta* **95** (1985) 287.
16. M. BERENYEI, in "Atlas of Thermoanalytical Curves", edited by G. Liptay (Heyden, 1973) p. 65.
17. S. St. J. WARNE and P. BAYLISS, *Amer. Mineral.* **47** (1962) 1011.
18. L. WALTER-LEVY and J. LANIEPCE, *Comp. Rend.* **250** (1960) 3320.
19. M. D. JUDD, B. A. PLUNKETT and M. I. POPE, *Thermal Anal.* **6** (1974) 555.
20. R. D. SHANNON and J. A. PASK, *J. Amer. Ceram. Soc.* **48** (1965) 391.
21. V. A. RUSSELL, *Thermochim. Acta* **19** (1977) 45.
22. M. TAKASHIGE, T. NAKAMURA, H. OZAWA, R. UNO, N. TSUYA and K. I. ARAI, *Jpn J. Appl. Phys.* **19** (1980) 255.
23. S. R. GURKOVICH and J. B. BLUM, *Ferroelectrics* **62** (1985) 189.

Received 23 November 1990
and accepted 10 April 1991